Scanning capacitance microscopy of AlGaN/GaN heterostructure field-effect transistor epitaxial layer structures

K. V. Smith and E. T. Yu[a)]
Department of Electrical and Computer Engineering, University of California, San Diego, La Jolla, California, 92093-0407

J. M. Redwing and K. S. Boutros
ATMI/Epitronics, 21002 North 19th Avenue, Suite 5, Phoenix, Arizona 85027-2726

(Received 6 July 1999; accepted for publication 12 August 1999)

Scanning capacitance microscopy is used to characterize local electronic properties in an $Al_xGa_{1-x}N$/GaN heterostructure field-effect transistor epitaxial layer structure. Lateral inhomogeneity in electronic properties is clearly observed, at length scales ranging from ~ 0.1 to >2 μm, in images obtained at fixed bias voltages. Acquisition of a series of images over a wide range of bias voltages allows local electronic structure to be probed with nanoscale spatial resolution both laterally and in depth. Combined with theoretical analysis of charge and potential distributions in the epitaxial layer structure under applied bias, these studies suggest that the dominant factor contributing to the observed variations in electronic structure is local lateral variations in $Al_xGa_{1-x}N$ layer thickness. © *1999 American Institute of Physics.* [S0003-6951(99)01441-2]

III–V nitride semiconductors are currently the subject of intense research for a variety of applications, including visible light emitters,[1] visible-blind ultraviolet photodetectors,[2] and high-temperature, high-power transistors[3–7] and diodes.[8] For heterostructure field-effect transistors (HFETs), the wide band gap, high breakdown field, high saturation velocity, and related material properties in nitride semiconductors have led to device demonstrations at very high power levels and microwave frequencies.[9–11] However, the epitaxial materials from which such devices are fabricated are typically characterized by high dislocation densities, local variations in composition and morphology, and a variety of defects that must ultimately be characterized, understood, and controlled.

In this letter we present studies of local electronic structure in an $Al_xGa_{1-x}N$/GaN HFET structure using scanning capacitance microscopy (SCM). This technique has been used extensively to perform dopant profiling in Si device structures,[12–14] and more recently to characterize local surface electronic structure in n-GaN epitaxial layers.[15] By acquiring and analyzing SCM images of $Al_xGa_{1-x}N$/GaN HFET epitaxial layers over a range of bias voltages, we have been able to observe variations in local electronic structure both laterally and in depth, and to determine the features in the structural morphology of the epitaxial layers from which these variations are most likely to arise.

The epitaxial layer structure used in these experiments, shown in Fig. 1, was grown by metal organic chemical vapor deposition (MOCVD) on a sapphire substrate. Following growth of a buffer layer, 3 μm of GaN and then 300 Å of $Al_{0.25}Ga_{0.75}N$ were grown. All layers were nominally undoped with a root-mean-square (rms) surface roughness of ~ 2 Å measured for a 1 μm$\times$1 μm area. Despite the absence of intentional doping, a two dimensional electron gas (2DEG) forms at the $Al_{0.25}Ga_{0.75}N$/GaN interface due to the presence of a large positive electrostatic sheet charge at the interface arising from spontaneous and piezoelectric polarization.[16–18] Hall measurements yield an electron sheet concentration of $\sim 5\times 10^{12}\,cm^{-2}$ and a mobility of ~ 1300 $cm^2/V\,s$ for this sample. The resulting energy-band-edge diagram and charge distribution are shown in Fig. 1.

A Digital Instruments 3100 atomic force microscope (AFM) with a scanning capacitance head was used to image the sample in the geometry indicated in Fig. 1. Imaging was performed in standard dC/dV open loop contact mode[17] using highly doped p^+ silicon tips coated with 50 Å of platinum to enhance tip conductivity. Electrical contact to the epitaxial layers was made using conductive silver tape. We have verified that the results described here do not depend on whether electrical contact is made in this manner directly to $Al_xGa_{1-x}N$ surface, or to a fully processed Ti/Al ohmic contact to the epitaxial layers. We relied on the native oxide present on the tip and the sample to minimize current flow during the SCM measurement. SCM images were acquired with an alternating-current (ac) bias of 1 V and direct-current (dc) bias voltages ranging from -6 to 6 V. For all SCM

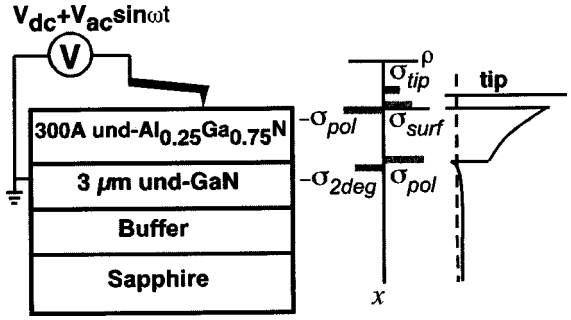

FIG. 1. (a) Schematic diagram of nominally undoped $Al_{0.25}Ga_{0.75}N$/GaN HFET showing geometry and electrical connections for SCM measurement. (b) Schematic of polarization-induced and free-carrier charge distribution. (c) Conduction-band diagram of tip/sample structure.

a)Electronic mail: ety@ece.ucsd.edu

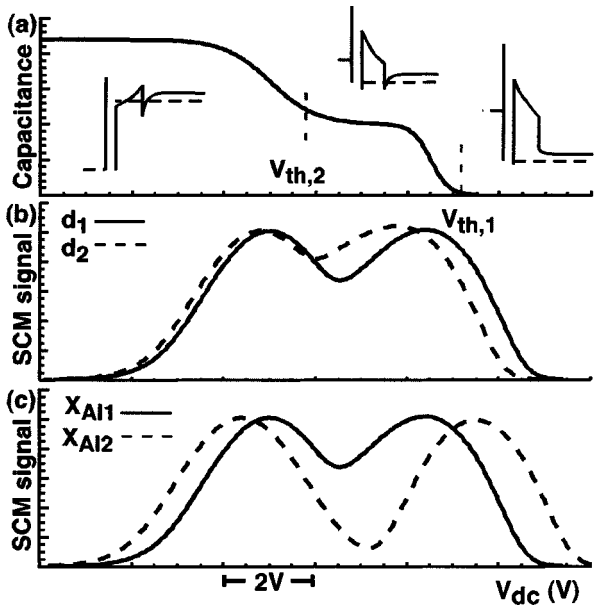

FIG. 2. (a) Model $C-V$ spectrum for an $Al_xGa_{1-x}N$/GaN HFET structure and conducting probe tip. Threshold voltages for 2DEG formation ($V_{th,1}$) and carrier spillover into the $Al_xGa_{1-x}N$ layer ($V_{th,2}$) are noted. Schematic energy-band diagrams for each constant capacitance region are also shown. Also shown are SCM signal spectra vs voltage calculated from model $C-V$ spectra for HFET structures with variations in (b) $Al_xGa_{1-x}N$ film thickness and (c) Al concentration within the $Al_xGa_{1-x}N$ barrier layer. Both capacitance and SCM signal are shown in arbitrary units.

images, contact mode AFM topographs are acquired simultaneously.

Figure 2(a) shows a schematic plot of the capacitance C between the tip and HFET structure under investigation, based on measured capacitance–voltage ($C-V$) characteristics for a large-area Schottky diode, as a function of dc bias voltage applied to the sample. For $V_{dc}>V_{th,1}$, the 2DEG is depleted and the capacitance is small. For $V_{th,2}<V_{dc}<V_{th,1}$, carriers are present primarily in the 2DEG and the sample capacitance is that of the $Al_xGa_{1-x}N$ barrier. For $V_{dc}<V_{th,2}$, carriers in the sample are present in the barrier and at the $Al_xGa_{1-x}N$ surface, leading to higher values for the capacitance. In the open-loop mode of operation, the SCM signal is proportional to dC/dV averaged over a voltage range $V_{dc}\pm V_{ac}$.[19] The resulting SCM signal calculated for the $C-V$ spectrum shown in Fig. 2(a) is indicated by the solid line in Fig. 2(b).

Contrast within the SCM images that we have obtained arises from local variations in electronic structure that may be associated with defects or with local inhomogeneities in the $Al_xGa_{1-x}N$ layer thickness or composition. The influence of such inhomogeneities on local electronic properties may be predicted via analytical calculations of the dependence of $V_{th,1}$ and $V_{th,2}$ on the $Al_xGa_{1-x}N$ layer thickness and composition. Following the general approach of Refs. 18 and 20, we obtain

$$V_{th,1}=-\phi_b+\frac{\Delta E_c-E_F}{e}+\frac{d}{\epsilon_{AlGaN}}\sigma_{pol}+\frac{t}{\epsilon_{gap}}\sigma_{surf}, \quad (1)$$

$$V_{th,2}=-\phi_b-\left(\frac{t}{\epsilon_{gap}}\right)\left(\frac{\epsilon_{AlGaN}}{d}\right)\left(\frac{\Delta E_c-E_F}{e}\right)-\frac{t}{\epsilon_{gap}}(\sigma_{pol}-\sigma_{surf}), \quad (2)$$

where ϕ_b is the metal–semiconductor Schottky barrier height, ΔE_c the $Al_xGa_{1-x}N$/GaN conduction-band offset, E_F the Fermi level, σ_{pol} the polarization charge, σ_{surf} the surface charge, d the $Al_xGa_{1-x}N$ layer thickness, t the thickness of the oxide present between the tip and sample, and ϵ_{AlGaN} and ϵ_{gap} the dielectric constants for the $Al_xGa_{1-x}N$ and oxide layers, respectively. From these equations it is then possible to determine the qualitative nature of contrast that will arise in the SCM images due to local variations in $Al_xGa_{1-x}N$ layer thickness and composition, and thereby to distinguish among features in local electronic structure arising from different aspects of nanoscale structure or composition.

Figures 2(b) and 2(c) show SCM signal spectra calculated for different $Al_xGa_{1-x}N$ layer thicknesses and compositions, respectively. From Fig. 2(b) we deduce that SCM contrast arising from a local variation in $Al_xGa_{1-x}N$ layer thickness will be inverted for $V_{dc}<V_{th,2}$ compared to that observed for $V_{dc}>V_{th,1}$. Conversely, we deduce from Fig. 2(c) that SCM contrast arising from a local variation in $Al_xGa_{1-x}N$ layer composition will be qualitatively similar (i.e., not inverted) for $V_{dc}<V_{th,2}$ and for $V_{dc}>V_{th,1}$. Thus, an analysis of the SCM image contrast over a range of dc bias voltages, rather than at a single voltage, will lead to insight into the physical origin—in addition to the presence—of local inhomogeneities in electronic structure.

Figure 3 shows $2.5\,\mu m\times 10\,\mu m$ topographic and SCM images of the $Al_{0.25}Ga_{0.75}N$/GaN HFET structure for dc bias voltages of -3 to 3 V. Corresponding locations in the topographic and SCM images are marked by symbols in the figure; from the AFM topographic images in Fig. 3, we see that some thermal drift has occurred during acquisition of these image sequences. A number of features in these images are noteworthy. For $V_{dc}=3$ V, the 2DEG is depleted and the contrast observed reflects primarily the electronic structure in the GaN layer. For $V_{dc}=2$ to 0 V, contrast associated with the formation of the 2DEG, i.e., local variation in the HFET threshold voltage, is observed. Substantial lateral variations in the threshold voltage are seen, with characteristic length scales of ~ 0.1 to >2 μm. In bulk semiconductors, the spatial resolution attainable in the SCM is typically limited by the Debye screening length and the probe tip size. For the HFET sample studied here, the spatial resolution near the HFET threshold voltage should be $\leqslant 0.1$ μm, limited by the probe tip size and $Al_xGa_{1-x}N$ layer thickness.

For $V_{dc}\leqslant -2$ V, carrier spillover into the $Al_xGa_{1-x}N$ barrier and toward the $Al_xGa_{1-x}N$ surface appears to occur. Within this range of voltages, one clearly sees that the SCM contrast is inverted compared to that observed for $V_{dc}=0$ to 2 V. As noted previously, this inversion of contrast is predicted to occur in the presence of threshold voltage inhomogeneities arising from $Al_xGa_{1-x}N$ layer thickness variations, and would not be expected if such inhomogeneities were to arise from local variations in $Al_xGa_{1-x}N$ composition. From this analysis we conclude that substantial local inhomogeneities in layer thickness, and consequently in threshold voltage, exist in the $Al_xGa_{1-x}N$/GaN HFET epitaxial layer structures characterized in these studies. These inhomogeneities are present at lateral length scales for which a substantial impact on the behavior of typical transistor structures fabricated from such material may occur. Preliminary calcula-

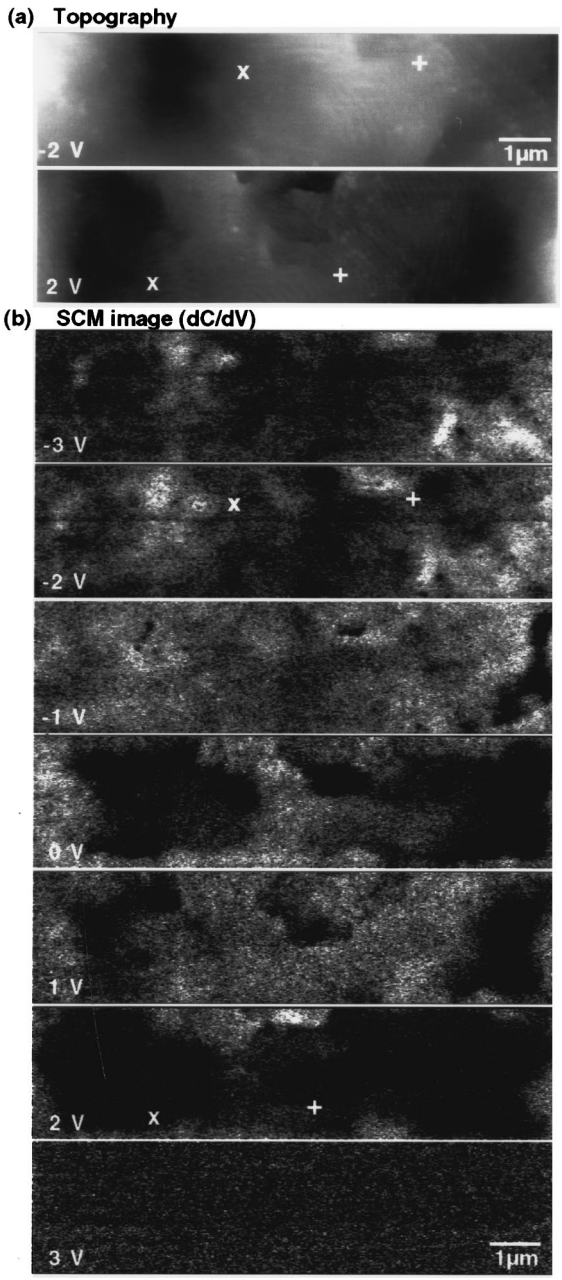

FIG. 3. (a) AFM topographic images and (b) simultaneously obtained SCM images of the $Al_{0.25}Ga_{0.75}N/GaN$ HFET structure. The sample-to-tip dc bias voltage is indicated for each image, and corresponding locations in the images obtained at $+2$ and -2 V are indicated by symbols.

tions indicate that the local threshold voltage can shift by several tenths of volts for a local variation in Al mole fraction of 0.05 or for a local variation in $Al_xGa_{1-x}N$ layer thickness of 50 Å.[21] A quantitative determination of the local threshold voltage shift present in this sample would require detailed analysis of local $C-V$ spectroscopic data.

In conclusion, we have used scanning capacitance microscopy to characterize nanoscale to submicron electronic properties of $Al_xGa_{1-x}N/GaN$ HFET epitaxial layer structures. By performing SCM imaging over a range of bias voltages, electronic structure both laterally and in depth has been probed. Such imaging combined with a detailed analysis of the relevant heterostructure device physics allows both the presence and possible physical origins of inhomogeneity in electronic structure to be ascertained. Substantial lateral variations in the threshold voltage for 2DEG formation has been observed in this manner; a theoretical analysis combined with SCM imaging over a range of bias voltages reveals that these variations appear to arise predominantly from inhomogeneity in the $Al_xGa_{1-x}N$ layer thickness.

The authors would like to acknowledge encouragement and technical assistance from H. Walker and W. McNeil of Dynamics Research Corp. Part of this work was supported by BMDO (Dr. Kepi Wu). E. T. Yu would like to acknowledge financial support from the Alfred P. Sloan Research Foundation.

[1] S. Nakamura, M. Senoh, S. Nagahama, N. Iwasa, T. Yamada, T. Matsushita, Y. Sugimoto, and H. Kiyoku, Appl. Phys. Lett. **70**, 1417 (1997).
[2] J. M. Van Hove, R. Hickman, J. J. Klaassen, P. P. Chow, and P. P. Ruden, Appl. Phys. Lett. **70**, 2282 (1997).
[3] M. A. Khan, Q. Chen, M. S. Shur, B. T. McDermott, J. A. Higgins, J. Burm, W. J. Schaff, and L. F. Eastman, IEEE Electron Device Lett. **17**, 584 (1996).
[4] O. Aktas, Z. F. Fan, A. Botchkarev, S. N. Mohammad, M. Roth, T. Jenkins, L. Kehias, and H. Morkoc, IEEE Electron Device Lett. **18**, 29 (1997).
[5] Y. F. Wu, B. P. Keller, S. Keller, D. Kapolnek, P. Kozodoy, S. P. DenBaars, and U. K. Mishra, Appl. Phys. Lett. **69**, 1438 (1996).
[6] G. J. Sullivan, M. Y. Chen, J. A. Higgins, J. W. Yang, Q. Chen, R. L. Pierson, and B. T. McDermott, IEEE Electron Device Lett. **19**, 198 (1998).
[7] S. C. Binari, J. M. Redwing, G. Kelner, and W. Kruppa, Electron. Lett. **33**, 242 (1997).
[8] Z. Z. Bandic, P. M. Bridger, E. C. Piquette, T. C. McGill, R. P. Vaudo, V. M. Phanse, and J. M. Redwing, Appl. Phys. Lett. **74**, 1266 (1999).
[9] Q. Chen, J. W. Yang, R. Gaska, M. Asif Khan, M. S. Shur, G. J. Sullivan, A. L. Sailor, J. A. Higgins, A. T. Ping, and I. Adesida, IEEE Electron Device Lett. **19**, 44 (1999).
[10] Y. F. Wu, B. P. Keller, N. X. Nguyen, M. Le, C. Nguyen, T. J. Jenkins, L. T. Kehias, S. P. DenBaars, and U. K. Mishra, IEEE Electron Device Lett. **18**, 438 (1997).
[11] S. T. Sheppard, K. Doverspike, W. L. Pribble, S. T. Allen, J. W. Palmour, L. T. Kehias, and T. J. Jenkins, IEEE Electron Device Lett. **20**, 161 (1999).
[12] C. C. Williams, J. Slinkman, W. P. Hough, and H. K. Wickramasinghe, Appl. Phys. Lett. **55**, 1662 (1989).
[13] D. W. Abrahams, C. Williams, J. Slinkman, and H. K. Wickramasinghe, J. Vac. Sci. Technol. B **9**, 703 (1991).
[14] C. J. Kang, C. K. Kim, J. D. Lera, Y. Kuk, K. M. Mang, J. G. Lee, K. S. Suh, and C. C. Williams, Appl. Phys. Lett. **71**, 1546 (1997).
[15] P. J. Hansen, Y. E. Strausser, A. N. Erickson, E. J. Tarsa, P. Kozodoy, E. G. Brazel, J. P. Ibbetson, U. Mishra, V. Narayanamurti, S. P. DenBaars, and J. S. Speck, Appl. Phys. Lett. **72**, 2247 (1998).
[16] A. Bykhovshi, B. Gelmont, and M. Shur, J. Appl. Phys. **74**, 6734 (1993).
[17] P. M. Asbeck, E. T. Yu, S. S. Lau, G. J. Sullivan, J. Van Hove, and J. Redwing, Electron. Lett. **33**, 1230 (1997).
[18] E. T. Yu, G. J. Sullivan, P. M. Asbeck, C. D. Wang, D. Qiao, and S. S. Lau, Appl. Phys. Lett. **71**, 2794 (1997).
[19] Digital Instruments Support Note No. 224, Rev. C, Digital Instruments, 1996 (unpublished), p. 224–225.
[20] E. T. Yu, X. Z. Dang, L. S. Yu, D. Qiao, P. M. Asbeck, S. S. Lau, G. J. Sullivan, K. S. Boutros, and J. M. Redwing, Appl. Phys. Lett. **73**, 1880 (1998).
[21] K. V. Smith and E. T. Yu (unpublished).